

Feeding methane vents and gas hydrate deposits at south Hydrate Ridge

Anne M. Tréhu,¹ Peter B. Flemings,² Nathan L. Bangs,³ Johanna Chevallier,¹ Eulàlia Gràcia,⁴ Joel E. Johnson,¹ C.-S. Liu,⁵ Xiaoli Liu,² Michael Riedel,⁶ and Marta E. Torres¹

Received 17 August 2004; revised 23 October 2004; accepted 10 November 2004; published 14 December 2004.

[1] Log and core data document gas saturations as high as 90% in a coarse-grained turbidite sequence beneath the gas hydrate stability zone (GHSZ) at south Hydrate Ridge, in the Cascadia accretionary complex. The geometry of this gas-saturated bed is defined by a strong, negative-polarity reflection in 3D seismic data. Because of the gas buoyancy, gas pressure equals or exceeds the overburden stress immediately beneath the GHSZ at the summit. We conclude that gas is focused into the coarse-grained sequence from a large volume of the accretionary complex and is trapped until high gas pressure forces the gas to migrate through the GHSZ to seafloor vents. This focused flow provides methane to the GHSZ in excess of its proportion in gas hydrate, thus providing a mechanism to explain the observed coexistence of massive gas hydrate, saline pore water and free gas near the summit. **INDEX TERMS:** 0915 Exploration Geophysics: Downhole methods; 0935 Exploration Geophysics: Seismic methods (3025); 5114 Physical Properties of Rocks: Permeability and porosity; 8145 Tectonophysics: Physics of magma and magma bodies. **Citation:** Tréhu, A. M., P. B. Flemings, N. L. Bangs, J. Chevallier, E. Gràcia, J. E. Johnson, C.-S. Liu, X. Liu, M. Riedel, and M. E. Torres (2004), Feeding methane vents and gas hydrate deposits at south Hydrate Ridge, *Geophys. Res. Lett.*, 31, L23310, doi:10.1029/2004GL021286.

1. Introduction

[2] Gas bubbles rise from gas hydrate mounds on the seafloor at Hydrate Ridge [Heeschen *et al.*, 2003], a peanut-shaped bathymetric high in the accretionary complex of the Cascadia subduction zone located 80 km west of Newport, Oregon (Figure 1a), and on other active and passive continental margins around the world [see Judd, 2003]. Free gas venting within the gas hydrate stability zone (GHSZ) is enigmatic because seafloor sediments are generally very porous and contain abundant water. Free gas should therefore be trapped within hydrate before reaching the seafloor. Several mechanisms have been proposed to explain this enigma, including formation of hydrate or oil

coatings around bubbles that form a barrier isolating the gas from the water [Suess *et al.*, 2001; Leifer and MacDonald, 2003], high pore water salinity that locally changes gas hydrate stability conditions, local dehydration of sediments, and inhibition of hydrate formation because of capillary forces [Ginsburg and Soloviev, 1997; Clennell *et al.*, 1999; Milkov *et al.*, 2004]. Modeling indicates that an abundant supply of gas is required to form massive gas hydrates and generate brines, which are formed when salts are excluded as hydrate forms [Torres *et al.*, 2004]. We show that gas saturations are high enough beneath the southern summit of Hydrate Ridge to form a critically pressured gas column beneath the GHSZ [Flemings *et al.*, 2003; Hornbach *et al.*, 2004] and drive gas migration through the GHSZ to the seafloor. Similar gas-rich conduits are probably present beneath other seafloor vents, but southern Hydrate Ridge is the only continental margin vent at which the data exist to resolve both conduit geometry and gas saturation.

2. Gas Saturation and Gas Pressure in Horizon A

[3] The key to understanding how gas hydrate and free gas can coexist in this system is to understand the plumbing beneath the GHSZ. One of the most striking features of a three-dimensional seismic survey of the region around southern Hydrate Ridge is an anomalously-bright, negative-polarity seismic reflection that we call Horizon A. Horizon A dips to the northeast from the summit and can be mapped over ~ 3 km² (Figures 1b–1d). Its western boundary is marked by a sharp decrease in amplitude where it enters the GHSZ. Along its eastern boundary, it terminates at an underlying unconformity. This unconformity separates older (>1.6 Ma), highly deformed accreted sediments from uplifted and folded slope-basin turbidites and hemipelagic sediments [Tréhu *et al.*, 2003]. The reflection amplitude is greatest beneath the summit and decreases sharply where it is deeper than ~ 1060 mbsl (meters below sea level) (Figure 1b). The strong amplitude, negative polarity, and down-dip decrease in amplitude that parallels structural contours suggest that free gas is present in the pore space above ~ 1060 mbsl.

[4] Data from ODP Leg 204 (Figure 1a) indicate that the Horizon A reflection originates at a 2–4 m thick zone that contains multiple coarse-grained, ash-rich turbidite beds (Figure 2a) [Tréhu *et al.*, 2003]. The in situ bulk density, as measured by logging while drilling (LWD), of this zone is low (1.25 – 1.46 g/cm³) compared to the bulk density of core samples (1.75 – 1.85 g/cm³) (Figures 2a and 2c). We interpret that free gas was present in the pores and that by the time the core was retrieved, the gas had escaped. Horizon A in situ gas saturations (S_g) (the volume fraction of pore space filled with gas) were estimated from measured

¹College of Oceanic and Atmospheric Sciences, Oregon State University, Corvallis, Oregon, USA.

²Department of Geosciences, Pennsylvania State University, University Park, Pennsylvania, USA.

³Institute for Geophysics, University of Texas at Austin, Austin, Texas, USA.

⁴Centre Mediterrani d'Investigacions Marines i Ambientals, UTM-CSIC, Barcelona, Spain.

⁵Institute of Oceanography, National Taiwan University, Taipei, Taiwan.

⁶Geological Survey of Canada, Sydney, British Columbia, Canada.

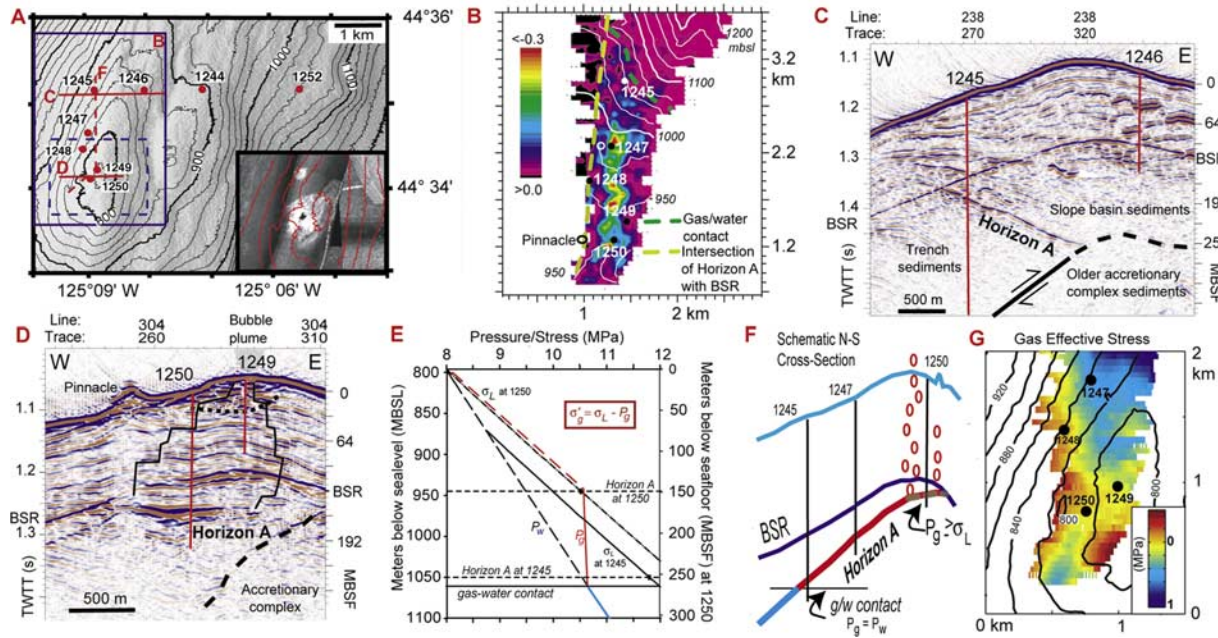


Figure 1. (a) Topography of southern Hydrate Ridge. ODP Leg 204 drill sites, and locations of Figures 1B–1E are shown. Dashed blue rectangle shows location of insert (lower right). Insert shows seafloor reflectivity at the summit [Johnson *et al.*, 2003] with topographic contours in red. (b) Reflection amplitude of Horizon A. White contours show the depth of this surface in meters beneath sea level (mbsl) (calculated assuming a constant velocity of 1486 m/s in the water and 1600 m/s in the sediments). The yellow dashed line shows the intersection of Horizon A with the bottom-simulating reflector (BSR), a reflection that indicates the base of the GHSZ and is caused by the impedance contrast between hydrate-bearing sediments and sediments containing free gas. The green dashed line shows the interpreted gas-water contact within Horizon A. To the west of the yellow dashed line, Horizon A amplitudes have limited extent and variable polarity, presumably as a result of hydrate, as opposed to gas, in the pores. Two dots for Site 1247 show Hole 1247A (solid circle), where LWD measurements were made, and Hole 1247B (open circle), where core samples were taken (Table 1). At other sites, cored holes were closer to the LWD hole. (c) EW seismic cross-section of the northern flank of south Hydrate Ridge. (d) EW cross-section through the summit. Dotted line shows the base of the shallow, massive gas hydrate deposit [Tréhu *et al.*, 2004]. Shaded area above the seafloor shows where bubbles have been observed in the ocean [Heeschen *et al.*, 2003]. No bubbles have been observed above the pinnacle. (e) Hydrostatic pressure (P_w), lithostatic stress (σ_L) and gas pressure (P_g) beneath the summit. P_w was calculated assuming a constant water density of 1.024 g/cm^3 ; P_g was calculated as discussed in the text; σ_L was calculated by integrating measured bulk densities downwards from the seafloor at each site and adding the load of the overlying water column. P_g and P_w do not vary laterally whereas σ_L varies as water depth and sediment density change. σ_L is shown for Sites 1245 and 1250. Above Horizon A at Site 1250, P_g is assumed to be parallel to σ_L (dashed red line), following Flemings *et al.* [2003]. (f) Schematic illustration of the model used to generate 1E. Ovals represent migrating free gas. (g) σ'_g in the summit region overlain by bathymetric contours. Contour interval is 20 m. An average velocity of 1577 m/s and an average density of 1740 kg/m^3 , as measured at Site 1250, were assumed for sediments above Horizon A. The uncertainty in σ'_g due to lateral variations in velocity (which range from 1550 to 1650 m/s based on multichannel seismic data [Bangs *et al.*, 2003]) is 0.15 MPa. The uncertainty due to lateral variations in density ($1699\text{--}1743 \text{ kg/m}^3$ based on LWD and MAD data at Sites 1247–1250 [Tréhu *et al.*, 2003]) is 0.06 MPa. The uncertainty due to uncertainty of $\sim 5 \text{ m}$ in water depth is 0.01 MPa.

densities assuming that the rock is a mixture of sediment grains, gas and water:

$$S_g = \frac{[\rho_b - \rho_s + \phi(\rho_s - \rho_w)]}{\phi(\rho_g - \rho_w)}.$$

The gas density (ρ_g) and the water density (ρ_w) were assumed to be 0.0628 g/cm^3 and 1.024 g/cm^3 , respectively. The bulk density (ρ_b) was derived from the LWD density measurements. The porosity (ϕ) and the grain density (ρ_s) were derived from shipboard moisture and density (MAD) core measurements. S_g in Horizon A is greater than 50% at all sites (Figure 3 and Table 1).

[5] When S_g exceeds a critical value, the gas forms an interconnected thread through the porous medium and flows as a separate phase. Experimental measurements suggest this critical value lies between 10 and 50% [Schowalter, 1979; England *et al.*, 1987]. Once free gas exists as an interconnected phase, it will flow under even small pressure gradients, and the gas pressure (P_g) will follow the gas density gradient as a function of depth. We estimate P_g in Horizon A by assuming that the decrease in amplitude beneath $\sim 1060 \text{ mbsl}$ marks the base of the connected gas column (the gas-water contact), where P_g equals the water pressure (P_w). We also assume that water pressure (P_w) equals the hydrostatic pressure and that the capillary entry pressure is negligible. Extrapolation of the gas pressure

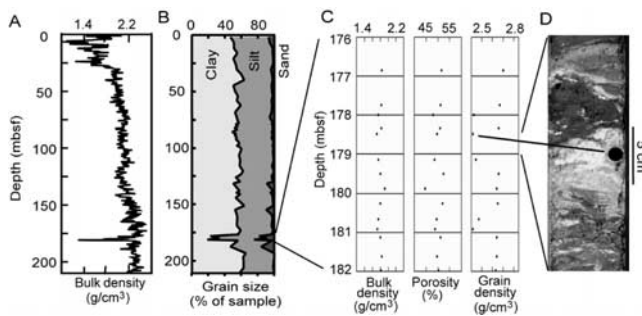


Figure 2. (a) In situ bulk density from logging while drilling (LWD) data at Site 1245. (b) Sediment grain size distribution at Site 1245. Grain size was measured using a Sedigraph 5100™ for particle sizes < 50 microns and a sedimentation tube for particles > 5 microns. (c) Moisture and density (MAD) measurements of bulk density, porosity and grain density for Horizon A at Site 1245. Samples showing low values of grain density are all from ash-rich layers. (d) Core image showing an ash-rich layer (interval 204-1245B-21P-2, 29–49 cm). Black circle and arrow indicate a sample taken for MAD measurements.

upward leads to the conclusion that P_g in Horizon A is approximately equal to the lithostatic stress (σ_L) at Site 1250, near the southern summit of Hydrate Ridge (Figure 1f). If the base of the connected gas column is deeper, or if pore waters are overpressured, the gas pressure will be even greater.

3. Discussion and Conclusions

[6] The vertical gas effective stress ($\sigma'_g = \sigma_L - P_g$) is low throughout the summit region (Figures 1e and 1g). When the effective stress is zero and the rock is weak, mechanical failure of the overlying rock should occur by hydraulic fracturing along planes perpendicular to the least principal stress; at somewhat lower pressures, slip on appropriately oriented pre-existing faults should occur [Finkbeiner *et al.*, 2001]. Minima in σ'_g indicate where free gas is most likely to escape from Horizon A by opening fractures. These minima occur where Horizon A enters the GHSZ beneath the pinnacle and where it onlaps the accretionary complex southwest of the summit (Figures 1d and 1g). We infer that free gas leaves Horizon A in this region and migrates towards the summit by opening vertical cracks and migrating laterally along relatively permeable strata. In convergent margins, the horizontal stress is generally thought to be greater than the vertical stress and horizontal hydraulic fractures might be expected. However, the presence of normal faults along the crest of Hydrate Ridge (for example, near Site 1246, Figure 1c) suggests an isotropic, or even tensional, stress state at the southern summit, which would lead to vertical hydraulic fractures. Two possible migration paths are shown schematically as fine black lines in Figure 1e. Actual migration paths probably vary temporally as well as spatially.

[7] Fluid mobility is proportional to relative permeability and inversely proportional to viscosity. The gas viscosity is much lower than the water viscosity, and the gas relative permeability is much higher than the water relative permeability because of the very high gas saturation. The flux of gas out of Horizon A will therefore greatly exceed the flux of water. Moreover, there is no driving force for water flow

if pore pressures are hydrostatic, whereas the driving force for buoyant gas, which is approximately the difference between the gas pressure in Horizon A and the hydrostatic pressure at the sea floor, is large.

[8] 5.75 moles of water are required for each mole of methane when hydrate is formed. At the pressure and temperature conditions at Hydrate Ridge, all pore water will be consumed by gas hydrate if gas fills more than 68% of the original fluid volume. Because the volume fraction of gas supplied is greater 68%, gas is being supplied in excess of the proportion of methane in hydrate. To convert all the gas to hydrate under these conditions, water must be drawn from the surrounding low permeability sediments [Ginsburg and Soloviev, 1997]. In very low permeability sediments, water supply will be limited and pore water salinity will rise as salt is excluded during hydrate formation. Moreover, if the salinity rises sufficiently, free gas will locally be thermodynamically stable within the hydrate stability zone [Milkov *et al.*, 2004]. Evidence for both sediment dehydration and high pore water salinity is found at Sites 1249 and 1250 [Tréhu *et al.*, 2003; Torres *et al.*, 2004].

[9] We conclude that venting at southern Hydrate Ridge is fed by the permeable and tabular Horizon A. This layer taps a large reservoir of hydrocarbon-rich fluids derived from older accreted and underplated sediments and also draws gas from the surrounding material because of its coarse grain size and resultant low capillary entry pressure [Schowalter, 1979]. We infer that formation of gas hydrate within the GHSZ sealed the conduit along its western edge, creating a trap. Free gas accumulated beneath this seal until it reached a critical thickness, which resulted in gas pressure high enough to dilate fractures and allow gas migration. Today, gas migrates through the GHSZ via a complex (and probably temporally variable) fracture network, driven by the high gas pressure gradient between Horizon A and the sea floor. One possible mechanism is suggested by the invasion/percolation model of Impey *et al.* [1997], which predicts that if the gas flow rate and the pressure difference

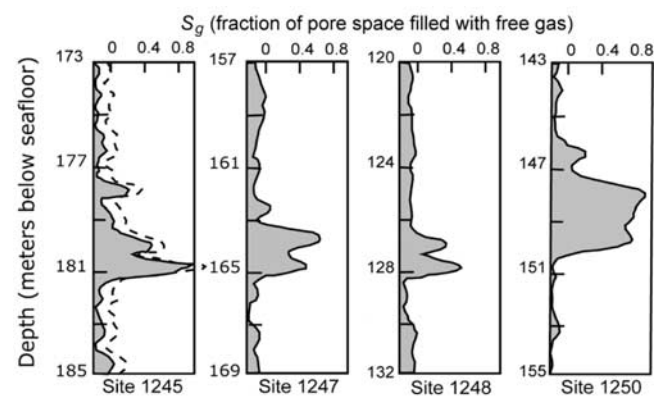


Figure 3. S_g calculated using ρ_b from LWD density logs and average ϕ and ρ_s from moisture and density (MAD) measurements made on samples from Horizon A (Table 1). Negative S_g outside Horizon A is an artifact of the anomalously low grain density of ash-rich layers in Horizon A. The dashed line for Site 1245 shows the effect of using $\rho_s = 2.65$ g/cm³, which excludes these low values. This higher value for ρ_s results in estimates for S_g that are close to 0 away from Horizon A but >1 in Horizon A.

Table 1. Parameters for Calculating the Percent of Gas Saturation in the Pore Space (S_g)^a

Site	Horizon A LWD Depth (mbsf)	ρ_b Min. LWD (g/cm ³)	ρ_b Ave. LWD (g/cm ³)	Horizon A Core Depth (mbsf)	ρ_s in Core (g/cm ³)	ϕ in Core	S_g Max. ^b	S_g Ave. ^b
1245	179.5–181.5	1.35	1.60	177.8–181.2	2.56	0.50	0.77	0.48
1247	163.5–165.5	1.44	1.59	not present ^c	(2.57)	(0.52)	0.68	0.38
1248	126.5–128.5	1.49	1.66	130–132	2.57	0.52	0.61	0.21
1250 ^d	147.5–150.5	1.25	1.36	147–150	2.6	0.55	0.91	0.71

^a S_g is shown for the minimum density in Horizon A (S_g max.) and for the average density over Horizon A (S_g ave.).

^bA perturbation of 0.02 in ϕ results in a change of 0.08 in S_g . A perturbation of 0.05 g/cm³ in grain density results in a change of 0.05 in S_g .

^cNo ash-rich horizon was observed in Hole 1247B. This hole was drilled 100 m west of 1247A, where the seismic character of Horizon A is distinctly different, suggesting that this local change in the seismic character of Horizon may result from a local change in lithology.

^dFew measurements are available from Horizon A at Site 1250 because of poor core recovery, probably because of high gas saturation.

between the gas source and outlet are high, steady gas flow will result; if they are low, gas flow will be intermittent. We speculate that this may be why gas expulsion is steady and less affected by changes in tidal pressure at southern Hydrate Ridge [Heeschen et al., 2003], in contrast to north Hydrate Ridge, where venting waxes and wanes with tidal and other periods [Torres et al., 2002].

[10] The plumbing system we describe provides a conceptual framework for understanding how gas passes from the free gas zone, through the hydrate stability zone, to be ultimately vented at the sea floor. A permeable conduit beneath the hydrate stability zone is needed to capture a significant amount of methane from a large volume in the subsurface. The conduit can result from lithologic variation, as at south Hydrate Ridge, or from creation of permeable fault gouge along a persistent fault. Formation of gas hydrate where the conduit enters the GHSZ should decrease the permeability, helping to trap gas within the conduit even if a conventional structural trap is absent. As gas saturation in the conduit increases, the gas forms a connected network. Eventually, gas pressure will increase enough to drive gas into the overlying low permeability sediments in the GHSZ. Given a sufficiently high gas flux and low sediment permeability, the gas will form hydrate, dehydrate the sediments, and elevate the salinity within the GHZ, ultimately creating local pathways in which free gas is stable. Whether gas flux is continuous or intermittent likely depends on gas flux beneath the GHSZ, the buoyant driving force, the strength of preexisting fractures, and the dynamics of stress-dependent permeability.

[11] **Acknowledgments.** We thank the Leg 204 Science Party, the ODP shipboard staff, and the crew of the JOIDES Resolution for the success of Leg 204. This research used data provided by the Ocean Drilling Program. The ODP is sponsored by the U.S. National Science Foundation (NSF) and participating countries under management of Joint Oceanographic Institutions (JOI), Inc. Funding for this research was provided by the National Science Foundation, the U.S. Science Support Program and the Penn State GeoFluidsII consortium.

References

- Bangs, N. L., I. Pecher, A. M. Tréhu, and Leg 204 Science Party (2003), Gas hydrate distribution and its relationship to free-gas sources within southern Hydrate Ridge: Results from recent seismic experiments (abstract), *Eos Trans. AGU*, 84(46), Fall Meet. Suppl., Abstract OS52C-01.
- Clenell, M. B., M. Hovland, J. S. Booth, P. Henry, and W. J. Winters (1999), Formation of natural gas hydrates in marine sediments: 1. Conceptual model of gas hydrate growth conditioned by host sediment properties, *J. Geophys. Res.*, 104, 22,985–23,003.
- England, W. A., A. S. MacKenzie, D. M. Mann, and T. M. Quigley (1987), The movement and entrapment of petroleum fluids in the subsurface, *J. Geol. Soc. London*, 144, 327–347.
- Finkbeiner, T., M. Zoback, B. B. Stump, and P. B. Flemings (2001), Stress, pore pressure and dynamically constrained hydrocarbon columns in the South Eugene Island 330 field, Gulf of Mexico, *AAPG Bull.*, 85, 1007–1031.
- Flemings, P. B., X. Liu, and W. J. Winters (2003), Critical pressure and multiphase flow in Blake Ridge gas hydrates, *Geology*, 31, 1057–1060.
- Ginsburg, G. D., and V. A. Soloviev (1997), Methane migration within the submarine gas-hydrate stability zone under deep-water conditions, *Mar. Geol.*, 137, 49–57.
- Heeschen, K. U., A. M. Tréhu, R. W. Collier, E. Suess, and G. Rehder (2003), Distribution and height of methane bubble plumes on the Cascadia margin characterized by acoustic imaging, *Geophys. Res. Lett.*, 30(12), 1643, doi:10.1029/2003GL016974.
- Hornbach, M. J., D. M. Saffer, and W. S. Holbrook (2004), Critically pressured free gas reservoirs below gas hydrate provinces, *Nature*, 427, 142–144.
- Impey, M. D., P. Grindrod, H. Takase, and K. J. Worgan (1997), A capillary network model for gas migration in low-permeability media, *SIAM J. Appl. Math.*, 57, 597–608.
- Johnson, J. E., C. Goldfinger, and E. Suess (2003), Geophysical constraints on the surface distribution of authigenic carbonates across the Hydrate Ridge region, *Mar. Geol.*, 202, 79–120.
- Judd, A. G. (2003), The global importance and context of methane escape from the seabed, *Geo Mar. Lett.*, 23, 147–154.
- Leifer, I., and I. MacDonald (2003), Dynamics of the gas flux from shallow gas hydrate deposits: Interaction between oily hydrate bubbles and the oceanic environment, *Earth Planet. Sci. Lett.*, 210, 411.
- Milkov, A. V., G. R. Dickens, G. E. Claypool, Y.-J. Lee, W. S. Borowski, M. E. Torres, W. Xu, H. Tomaru, A. M. Tréhu, and P. Schultheiss (2004), Co-existence of gas hydrate, free gas, and brine within the gas hydrate stability zone at the southern summit of Hydrate Ridge (Oregon margin): Evidence from prolonged degassing of a pressurized core, *Earth Planet. Sci. Lett.*, 222, 829–843.
- Schowalter, T. T. (1979), Mechanics of secondary hydrocarbon migration and entrapment, *AAPG Bull.*, 63, 723–760.
- Suess, E., et al. (2001), Seafloor methane hydrates at Hydrate Ridge, Cascadia margin, in *Natural Gas Hydrates: Occurrence, Distribution and Detection*, *Geophys. Monogr. Ser.*, vol. 124, edited by C. K. Paull and W. P. Dillon, pp. 87–98, AGU, Washington, D. C.
- Torres, M. E., J. McManus, D. E. Hammond, M. A. de Angelis, K. U. Heeschen, S. L. Colbert, M. D. Tryon, K. M. Brown, and E. Suess (2002), Fluid and chemical fluxes in and out of sediments hosting methane hydrate deposits on Hydrate Ridge, OR, I: Hydrological provinces, *Earth Planet. Sci. Lett.*, 201, 525–540.
- Torres, M. E., K. Wallmann, A. M. Tréhu, G. Bohrmann, W. S. Borowski, and H. Tomaru (2004), Gas hydrate dynamics at the Hydrate Ridge southern summit based on dissolved chloride data, *Earth Planet. Sci. Lett.*, 226, 225–241.
- Tréhu, A. M., et al. (2003), *Proceedings of the Ocean Drill. Program Initial Report* [CD-ROM], vol. 204, Ocean Drill. Program, Texas College Station, Tex.
- Tréhu, A. M., et al. (2004), Three-dimensional distribution of gas hydrate beneath southern Hydrate Ridge: Constraints from ODP Leg 204, *Earth Planet. Sci. Lett.*, 222, 845–862.
- N. L. Bangs, Institute for Geophysics, University of Texas at Austin, Austin, TX 78759–8500, USA.
- J. Chevallier, J. E. Johnson, M. E. Torres, and A. M. Tréhu, College of Oceanic and Atmospheric Sciences, Oregon State University, Corvallis, OR 97331, USA. (trehu@coas.oregonstate.edu)
- P. B. Flemings and X. Liu, Department of Geosciences, Pennsylvania State University, University Park, PA 16802, USA.
- E. Gràcia, Centre Mediterrani d'Investigacions Marines i Ambientals, UTM-CSIC, E-08003 Barcelona, Spain.
- C.-S. Liou, Institute of Oceanography, National Taiwan University, Taipei 106, Taiwan.
- M. Riedel, Geological Survey of Canada, Sidney, BC, Canada V8L 4B2.